International Journal of Advances in Applied Sciences (IJAAS)
Vol. 15, No. 2, June 2026, pp. 760~774
ISSN: 2252-8814, DOI: 10.11591/ijaas.v15.i2.pp760-774

A novel multi-terminal fuzzy-logic controlled IUPQC device for power quality enhancement in multi-feeder distribution systems

Venna Jaya Lakshmi[1], Katragadda Swarnasri[2]
[1]Department of Electrical and Electronics Engineering, Acharya Nagarjuna University, Guntur, India
[2]Department of Electrical and Electronics Engineering, RVR & JC College of Engineering, Guntur, India

Article Info

Article history:

Received Jul 15, 2025
Revised May 13, 2026
Accepted May 23, 2026

Keywords:

Fuzzy-logic controller
Multi-feeder distribution system
Multi-terminal IUPQC topology
Power quality enhancement
Total-harmonic distortions

ABSTRACT

Non-linear sensitive loads are increasingly being used in a wide range of industrial and home applications. Particularly, some nonlinear sensitive loads degrade the power quality (PQ) of a multi-feeder distribution system by causing current as well as voltage quality to deviate from normal standards. To address these PQ issues, a unique multi-terminal interline-unified power quality conditioner (MT-IUPQC) device has been implemented in a multi-feeder distribution system. This MT-IUPQC is made up of multi-voltage source inverters (VSI) coupled by a common direct current (DC)-linked capacitor, and which is controlled by using proportional integral (PI) control method. However, due to an inappropriate gain setting choice, this PI is not suitable for regulating the DC voltage at the specified voltage level. In this paper, an intelligent fuzzy-logic controlled MT-IUPQC provides an intelligent knowledge set with subjective assessments for improved mitigation of PQ difficulties. The recovered total harmonic distortion (THD) of source current is 2.45%, 2.71%, which are well within IEEE-519/2014 norms and significantly lower than the THD of non-linear sensitive load current of 30.19%, 30.05% in both feeder-1 and 2. In a similar way, the THD of non-linear sensitive load voltage is obtained at 0.43%, which fits well under IEEE-519/2014 norms and is significantly lower than the THD of the voltage source measured at 20.62% in feeder-1.

Corresponding Author:

Venna Jaya Lakshmi
Department of Electrical and Electronics Engineering, Acharya Nagarjuna University
Namburu, Guntur, Andhra Pradesh, India
Email: vennajayalakshmi.eee@gmail.com

1. INTRODUCTION

Power quality (PQ) has emerged as an essential necessity for a power distribution network's effective operation. Distribution networks are extremely vulnerable to power outages and supply disruptions due to their interconnections with multiple-load equipment [1]. Consequently, a variety of PQ issues have an impact on sensitive loads in power distribution networks. According to various research studies on PQ problems, loads account for 68% of PQ matters, while the grid-utility system accounts for 32%. PQ refers to consistency and effectiveness, which are impacted by voltage quality and current quality at the end-user level. The PQ is ideally referred to as a pure sinusoidal source voltage with a steady magnitude and fundamental of their frequency. Because of current and voltage imperfections in the common point of the distribution system, severe techno-economic impacts have been observed [2].

Numerous conditions that arise in highly sensitive loads and result in loss of ability and efficiency are utilized to recognize PQ concerns in the electric distribution supply network. Effective PQ detection methodologies should be employed to determine the nature of the PQ concern impacting the system, and robust

monitoring systems are required [3]. The purpose of this research is to minimize the amount of PQ difficulties that arise in multi-feeder distribution systems, including voltage/current harmonics, voltage interruptions, voltage sags/swells, frequency deviations, unbalanced voltage, load unbalanced, and reactive-power drop.

Owing to this perspective, several professional scientists and investigators are driven to build complex PQ enhancement approaches known as customized power compensation (CPC) technology [4]. Singh and Letha [5] describe a number of possible circumstances for compensation of PQ issues by adopting the series/shunt interconnected compensating systems. Such a CPC system recruits the customized-power devices (CPDs) to compensate any current and/or voltage-specific PQ concerns, resulting in the multi-feeder system becoming sinusoidal in nature, linearly balanced, and fundamental factor [6]. Several multi-feeders CPD techniques [7]–[10] are reported in literature; these compensatory techniques operate individually to resolve voltage or current-driven PQ concerns [11], [12]. Along with classical CPD strategies discussed above, the multi-terminal driven interlined unified power-quality compensator (MT-IUPQC) is being developed to handle any voltage and/or current-driven PQ concerns in a multi-feeder distribution network. Additionally, it can transmit reactive power across the feeders in immediate form while providing uninterrupted power delivery to customers throughout power failures.

The suggested MT-IUPQC system is made up of numerous voltage source inverters (VSIs) coupled in a shunt/series configuration and driven by a usual direct current (DC) link. The voltage is maintained at a sufficient threshold value. This MT-IUPQC addresses simultaneous load-related and source-related PQ concerns in a three-phase medium frequency (MF) distribution network by employing well-functioning control algorithms to obtain voltage and current reference values by monitoring the source and load-side specifications. In general, the synchronous reference frame (SRF) controller [13] is being employed to calculate the voltage reference corresponding to a series-connected MT-IUPQC apparatus. Similarly, the instantaneous real-power (IRP) controller [14] is being employed to calculate the current reference to the shunt-connected MT-IUPQC apparatus. But, the above SRF/IRP controller utilizes the proportional integral (PI) controller for DC-link voltage regulation at a specified reference DC voltage level [15]–[21]. The major problem is identified in PI control, due to inappropriate gain setting choice; this PI is not suitable for providing suitable gain values because of parameter variations, load situations, and time-varying functions. The main aim of this work is to regulate the DC voltage at a specified voltage level by using an intelligent fuzzy-logic controller (FLC), which provides the intelligent knowledge set with subjective assessments for improved mitigation of PQ difficulties. In this work, the working and performance of the FLC-controlled SRF/IRP-controlled the MT-IUPQC device is verified by using the MATLAB/Simulation platform the outcome results are illustrated with suitable comparisons.

2. COMPENSATION METHODOLOGY

The multi-feeder active compensation systems are the most tailored compensation approaches for addressing diverse PQ challenges in multi-feeder distribution networks. It addresses a combination of voltage and current-driven PQ concerns in a multi-feeder system. Actually, it has the ability to shift reactive and actual power across its own and nearby feeds, assuring continuous power transfer to neighbor loads regardless of any abrupt interruptions [22]. The block diagram of the MT-IUPQC device is illustrated in Figure 1.

It consists of four VSIs connected as a shunt/series combination and interconnected at the point of common coupling (PCC) of a multi-feeder distribution network driven by a common DC-link capacitor (CDC), which are interfaced to a multi-feeder network by using a 1:1 linear transformer. The shunt VSIs-2 and 4 helps to mitigate any current-driven PQ concerns like current harmonics, reactive-power regulation, load sharing/balancing, and also maintain unity-power factor in both feeder-1 and 2, which are operated as in-phase opposition compensation principle. Similarly, the series VSIs-1 and 3 helps to mitigate any voltage-driven PQ concerns like voltage harmonics, voltage interruptions, voltage sags-swells, and also maintains the voltage profile in both feeders-1 and 2, which are operated as a direct-compensation principle [23].

In this way, the proposed MT-IUPQC device is always dependent on obtaining possible reference currents/voltages via substantial control schemes. Such control schemes obtain reference current/voltage signals from distorted source voltages and currents of their respective feeders via sensing elements. Some of the well-known control schemes are the SRF and IRP control schemes for both voltage/current compensation methodologies. In general, the SRF controller is employed to calculate the voltage reference corresponding to the series-connected VSI-1 and 3 of the MT-IUPQC apparatus. Similarly, the IRP controller is being employed to calculate the current reference to shunt-connected VSIs-2 and 4 of the MT-IUPQC apparatus. The obtained reference voltages and currents are used to control the switching actions of the MT-IUPQC device VSIs initiated by gate-pulse generation units [24].

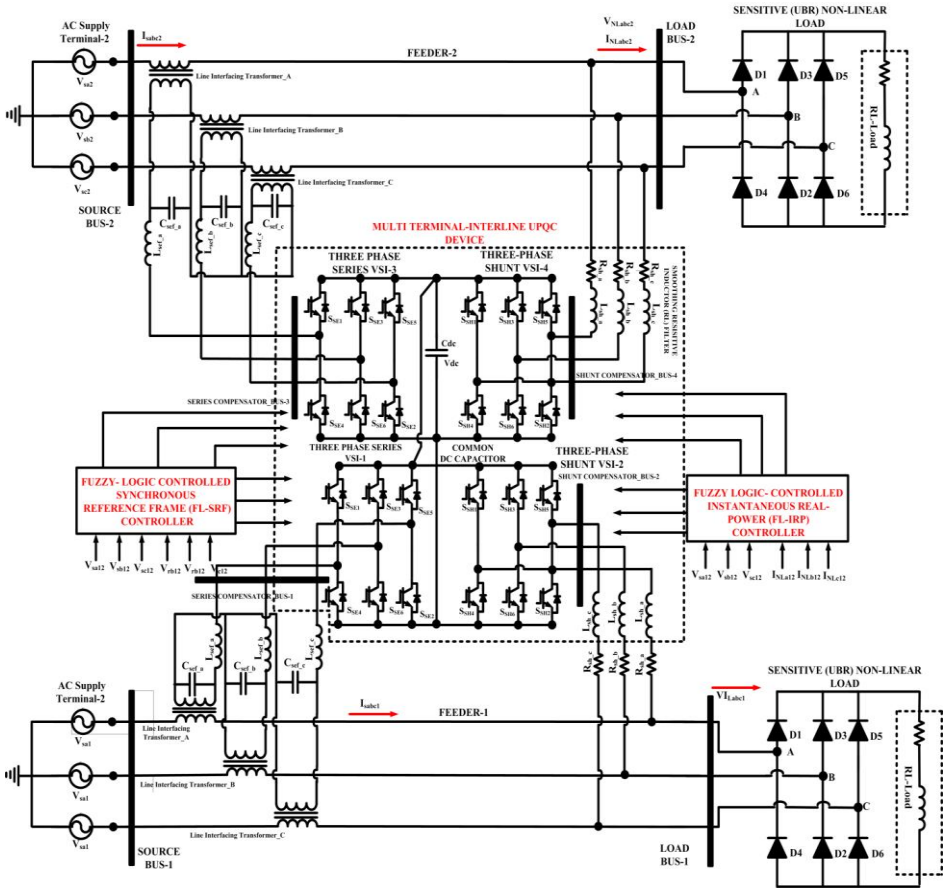

Figure 1. Schematic diagram of MT-IUPQC topology for PQ enhancement

By using Park's conversion technique, the production of reference voltage signals is extracted by comparing the transformed actual and reference voltage vectors in the dq-axis. This comparator produces some error quantities. These error values have been minimized for getting a perfect voltage vector by using a PI controller with proper selection of $(Kp.s)$ and $(Ki.s)$ through the Ziegler-Nichols method. The voltage controller's transfer function is as (1) and (2).

$$V_{err}(s) = \left(k_{p.s} + \frac{k_{i.s}}{s}\right) \times E_{err}(s) \quad (1)$$

$$\Delta V_{err}(s) = V_{err}(s) - V_{err}(s-1) \quad (2)$$

Where $V_{err}(s)$ and $\Delta V_{err}(s)$ are the error and the change in error.

The major problem is identified in PI control, due to inappropriate gain setting choice; this PI is not suitable for providing suitable gain values because of parameter variations, load situations, and time-varying functions. An intelligent fuzzy logic controller (FLC) is most relevant when the inference system is symbolically modelled, and considerable expert knowledge is applied [25]. This FLC exemplifies an intelligent, knowledge-driven process that includes FLC membership functions and fuzzy logic rule structure. These FLC-membership functions and FLC rules are essential components of fuzzy controllers, converting critical relevant judgments from human knowledge data to artificial knowledge data [26]. Several attempts are made to understand the needed fulfillment in system performance using the fantastic learning technique to calculate the relationship between FLC rules and FLC membership functions. The structure of FLC is shown in Figure 2. The fuzzy inference method illustrates how the FLC is produced by employing confident logical actions and a knowledge base of "IF and THEN" from diverse language logical operations [27].

The FLC membership functions and FLC rule-structure for elimination of error components by utilizing expertise intelligence knowledge are clearly shown in Figure 3 and Table 1. The block diagram of the proposed FLC-SRF controller is presented in Figure 4. The seven FLC-MF'S are used and defined as positive small (PS), negative small (NS), positive medium (PM), negative medium (NM), positive big (PB), negative big (NB), and zero (ZE), accordingly.

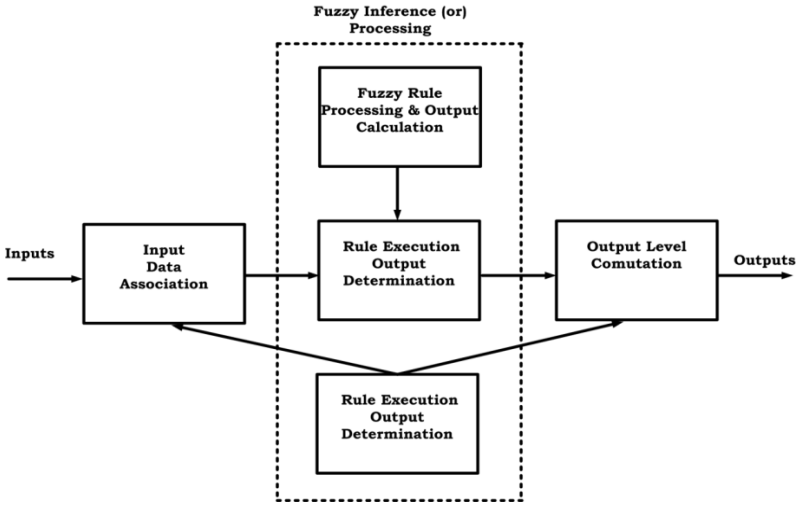

Figure 2. Structure of FLC

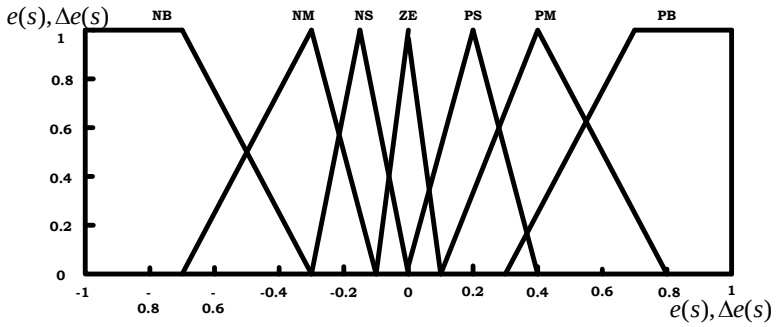

Figure 3. FLC membership functions

Table 1. FLC rule structure

$err\ (s)$ / $\Delta err\ (s)$	NB	NM	NS	ZE	PS	PM	PB
NB	NB	NM	NS	NB	NM	NS	ZE
NM	NM	NS	NB	NM	NS	ZE	PS
NS	NS	NB	NM	NS	ZE	PS	PM
ZE	NB	NM	NS	ZE	PS	PM	PB
PS	NM	NS	ZE	PS	PM	PB	PB
PM	NS	ZE	PS	PM	PB	PB	PB
PB	ZE	NM	NS	ZE	PS	PM	PB

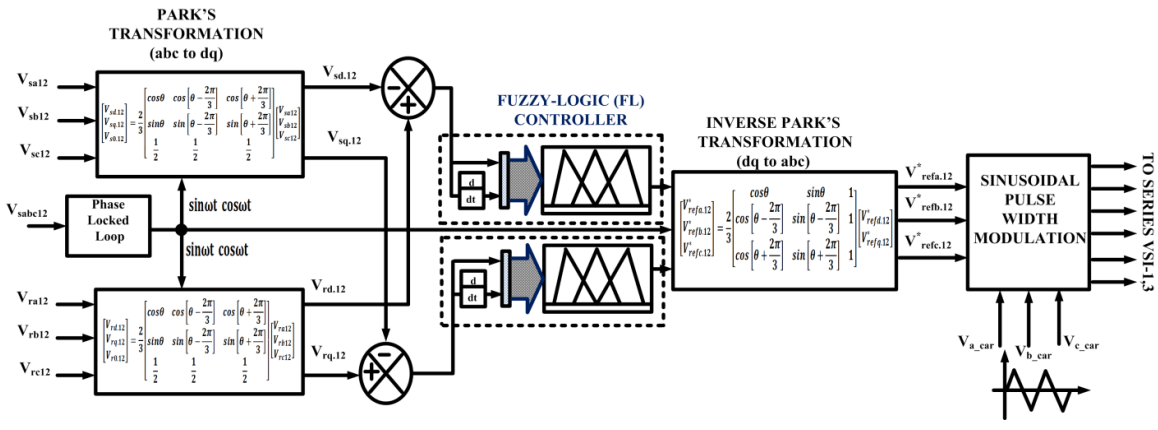

Figure 4. Block diagram of FLC-SRF controller

Thus, the obtained error quantities are minimized by using the FLC-SRF controller, which helps to produce the feasible voltage reference in the dq-frame, which is retransformed into the abc-frame by using inverse-Park's conversion method, and the final voltage reference signal is described in (3).

$$\begin{bmatrix} V^*_{refa.12} \\ V^*_{refb.12} \\ V^*_{refc.12} \end{bmatrix} = \frac{2}{3}\begin{bmatrix} cos\theta & sin\theta & 1 \\ cos\left[\theta - \frac{2\pi}{3}\right] & sin\left[\theta - \frac{2\pi}{3}\right] & 1 \\ cos\left[\theta + \frac{2\pi}{3}\right] & sin\left[\theta + \frac{2\pi}{3}\right] & 1 \end{bmatrix}\begin{bmatrix} V^*_{refd.12} \\ V^*_{refq.12} \end{bmatrix} \quad (3)$$

Similarly, using Clarke's conversion technique produces the reference current signals, which are extracted by comparing the transformed actual and reference current components in a symmetrical orthogonal coordinate. The attained current components are propagated to a second-order high-pass filter to allow higher-order frequencies for better generation of reference currents. Along with reference to the current generation, the FLC-IRP controller maintains the DC-link voltage as constant with a specified voltage value by comparing the actual DC-link ($V_{dc.c}$) and specified DC-link voltage value ($V^*_{dc.r}$) by eliminating the error quantities (4) and (5).

$$V_{dc.cer} = V^*_{dc.r} - V_{dc.c} \quad (4)$$

$$\Delta_{ia.dc} = K_{p.d} * \left(V_{dc.cer(n)} - V_{dc.cer(n-1)}\right) + K_{i.d} * \left(V_{dc.cer(n)}\right) \quad (5)$$

This FLC exemplifies an intelligent knowledge-driven process that includes FLC membership functions and a FLC rule structure is essential components of fuzzy controllers for producing robust performance. The block diagram of the proposed FLC-IRP controller is depicted in Figure 5. Thus, the obtained error quantities are minimized by using FLC-IRP controller, which helps to produce the feasible current reference in $\alpha\beta$-frame, which is retransformed into abc by using inverse-Clarke's conversion method, and the final current reference signal is described in (6).

$$\begin{bmatrix} i^*_{cr.a12} \\ i^*_{cr.b12} \\ i^*_{cr.c12} \end{bmatrix} = \sqrt{\frac{2}{3}}\begin{bmatrix} 1/\sqrt{2} & 1 & 0 \\ 1/\sqrt{2} & -1/2 & \sqrt{3}/2 \\ 1/\sqrt{2} & -1/2 & -\sqrt{3}/2 \end{bmatrix}\begin{bmatrix} i^*_{c.012} \\ i^*_{c.\alpha 12} \\ i^*_{c.\beta 12} \end{bmatrix} \quad (6)$$

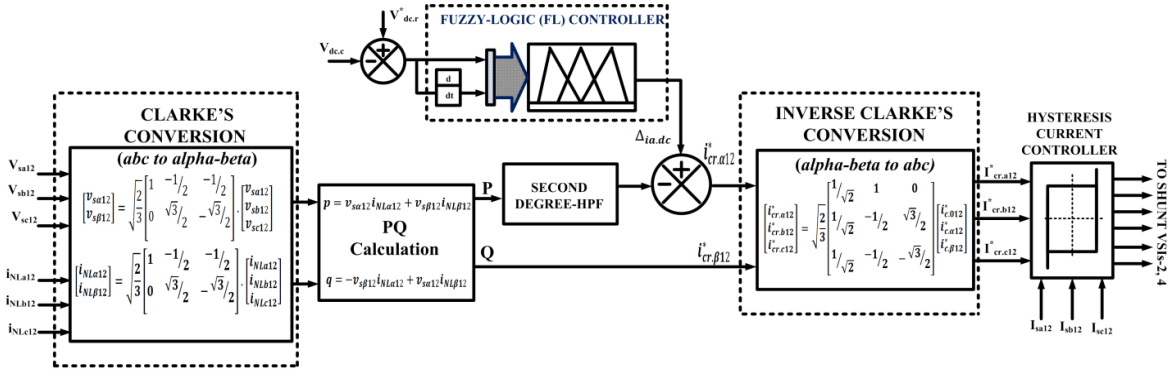

Figure 5. Block diagram of FLC-IRP controller

So finally, the extracted reference voltages from FLC-SRF controller are propagated with the actual voltage signal for generation of feasible switching states to series VSIs-1 and 3 of MT-IUPQC device. This is done by employing the sinusoidal pulse-width modulation. Similarly, the extracted reference currents from FLC-IRP controller are propagated with the actual source current for generation of feasible switching states to shunt VSIs-2 and 4 of MT-IUPQC by employing the hysteresis current controller-based gate-driver circuitry.

3. DISCUSSION OF MATLAB/SIMULINK RESULTS

In this work, the working and performance of the FLC-controlled SRF/IRP-controlled MT-IUPQC device is verified by using the MATLAB/Simulation platform. The specifications used in the simulation model are presented in Table 2. These specifications serve as the basis for evaluating the effectiveness of the proposed controller.

Table 2. Simulation specifications

S. No	Parameters	Values Feeder-1 and 2
1	Three-phase source voltage (V_{rms})	V_{sabc12}-415 V, 50 Hz
2	Line impedance	R_{s12} =0.15 Ω, L_{s12}-0.9 mH
3	Sensitive load impedances	R_L =30 Ω, L_L-20 mH (NL-load)
4	Linear (1:1) transformer	415 V, 50 Hz, linear model -5 KVA, 10% leakage reactance
5	Series-connected VSIs-1 and 3 filters	L_{se}-3 mH, C_{se}-100 µF
6	Shunt-connected VSIs-2 and 4 filters	R_{sh} =0.001 Ω, L_{sh}-10 mH
7	Common DC-link capacitor	$V_{dc.c}$ =880 V, $C_{dc.c}$ =1500 µF

3.1. Compensation of voltage or current concerns in feeder-1 using FLC-based SRF/IRP-controlled MT-IUPQC device

The simulation outcomes of current compensation in feeder-1 using FLC-based IRP-controlled VSI-2 of MT-IUPQC device is depicted in Figure 6. In this case, the feeder-1 of the multi-feeder distribution network is energized with a voltage of 415 Vrms, 50 Hz for driving the sensitive non-linear load. This sensitive non-linear load produces the uneven harmonic currents into the PCC of feeder-1. Due to these harmonic distortions, feeder-1 has been damaged and loss of control in the system. Then the shunt VSI-2 of MT-IUPQC in feeder-1 mitigates the harmonic distortions in source current, which is operated as in-phase opposition compensation principle is shown in Figure 6. Figure 7 shows the current total harmonic distortion (THD) spectrum analysis in feeder-1. The THD of the non-linear sensitive load current of 30.19% in feeder-1 is shown in Figure 7(a), while the recovered THD of the source current is 2.45% as shown in Figure 7(b), which is well within IEEE-519/2014 norms. The FLC-IRP controller always maintains DC-link voltage as the specified voltage value of 880 V is depicted in Figure 8, and also the source current of feeder-1 is always in-phase with the source voltage, which represents the unity power-factor is shown in Figure 9.

The simulation outcomes of voltage compensation in feeder-1 using FLC-based SRF-controlled VSI-1 of MT-IUPQC device are depicted in Figure 10. In this case, the feeder-1 of the multi-feeder distribution network is energized with a voltage of 415 Vrms, 50 Hz for driving the sensitive non-linear load. This sensitive non-linear load produces the uneven harmonic currents, which cause the voltage harmonics in feeder-1 and damage the entire load apparatus. Then the series VSI-1 of MT-IUPQC in feeder-1 mitigates the voltage harmonics in load voltage, which is operated as a direct compensation principle, as shown in Figure 10. Figure 11 shows the voltage THD spectrum analysis in feeder-1: the THD of source voltage is 20.62% as in Figure 11(a), and the recovered THD of sensitive load voltage is 0.43% as in Figure 11(b), which is well within IEEE-519/2014 norms. Similarly, the VSI-1 of MT-IUPQC mitigates the voltage sag, voltage swell, and voltage interruptions in feeder-1 are shown in Figures 12 to 14, respectively. The obtained results show that the feeder-1 becomes sinusoidal in nature, linearly, balancing and fundamental factor, and delivers the quality-power and reliable power to consumer loads.

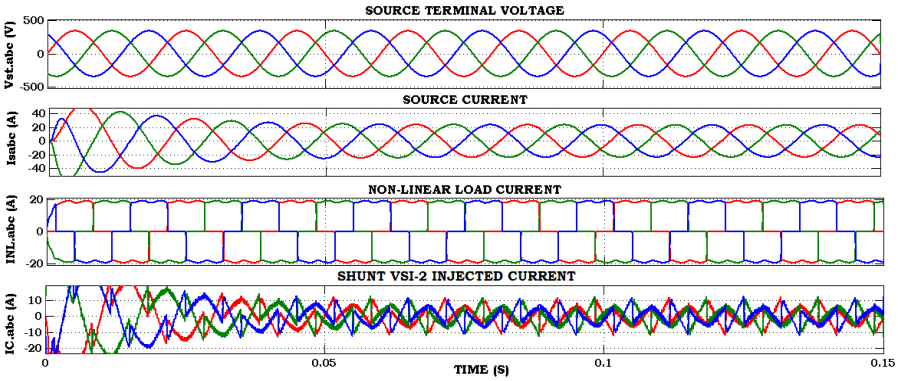

Figure 6. Simulation outcomes of current compensation in feeder-1 using FLC-based IRP-controlled VSI-2 of the MT-IUPQC device

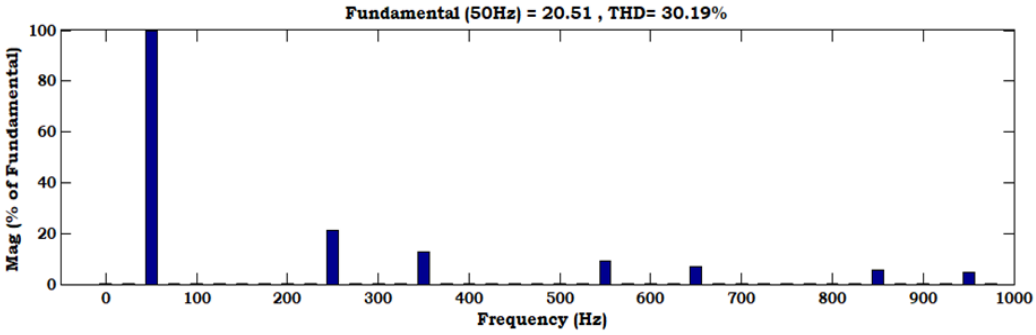

(a)

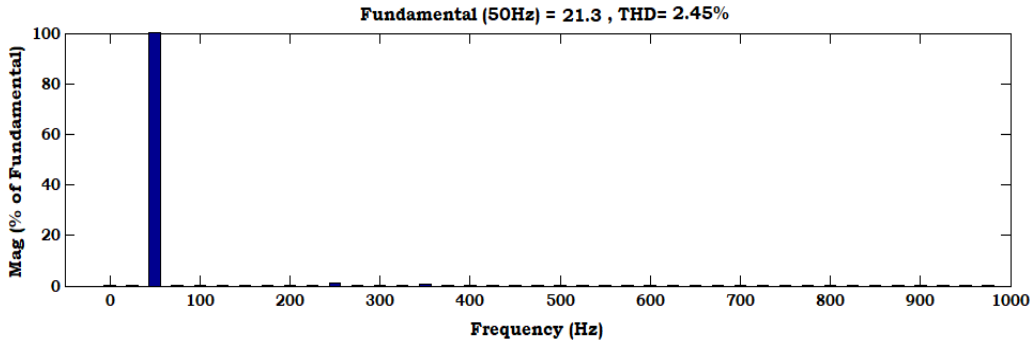

(b)

Figure 7. Current THD spectrum analysis in feeder-1 (a) THD of non-linear sensitive load current and (b) THD of source current

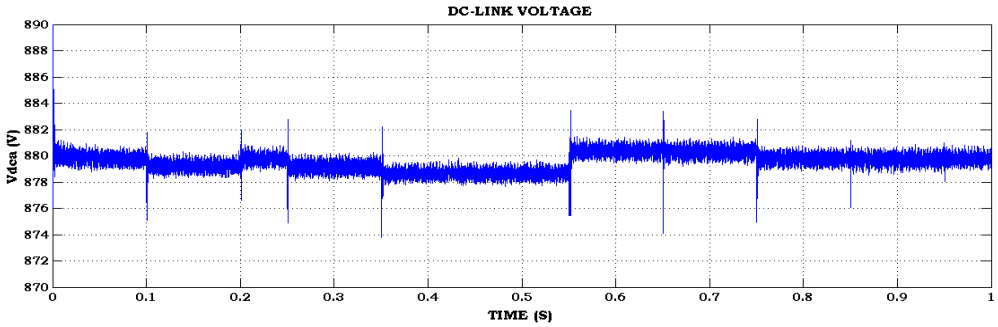

Figure 8. DC-link capacitor voltage

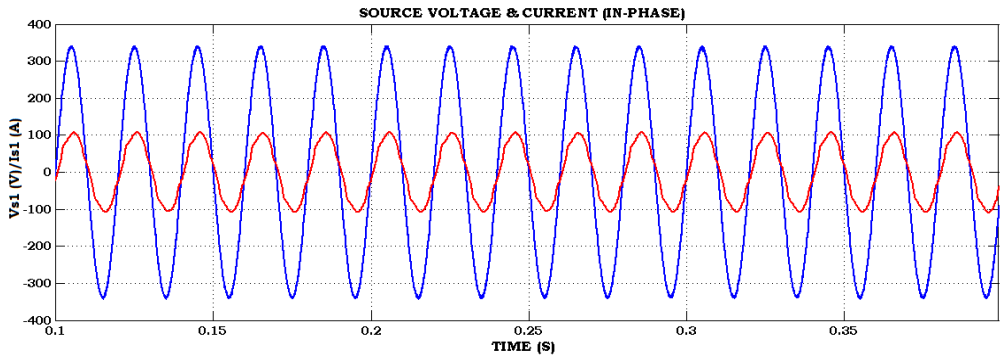

Figure 9. Source voltage and current (in-phase)

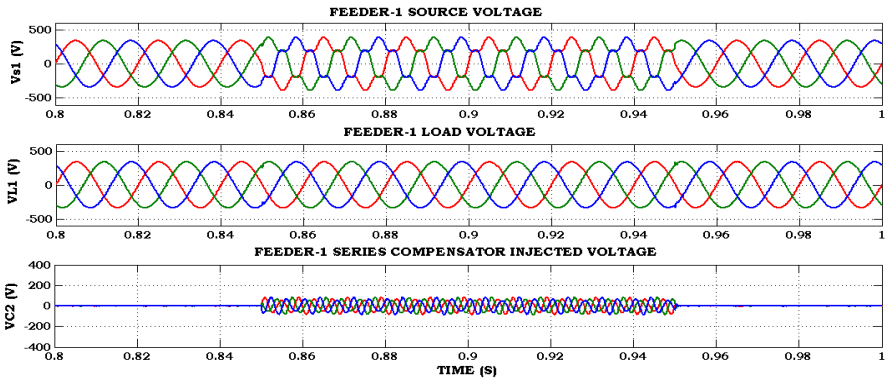

Figure 10. Simulation outcomes of voltage compensation in feeder-1 using FLC-based SRF-controlled VSI-1 of the MT-IUPQC device

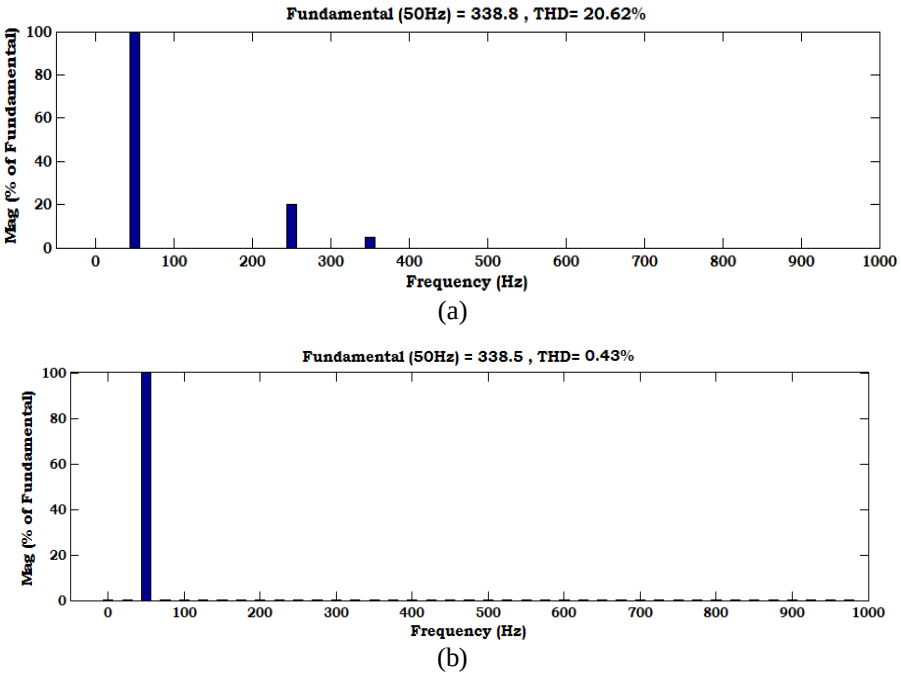

Figure 11. Voltage THD spectrum analysis in feeder-1 (a) THD of source voltage and (b) THD of sensitive non-linear load voltage

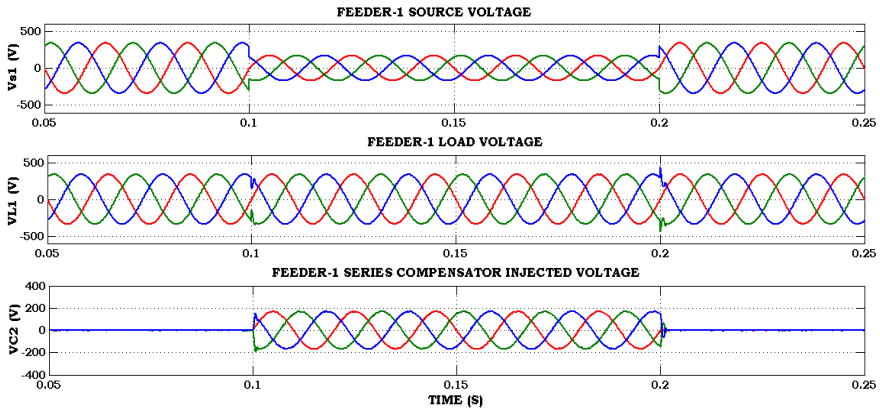

Figure 12. Simulation outcomes of voltage-sag compensation in feeder-1 using FLC-based SRF-controlled VSI-1 of the MT-IUPQC device

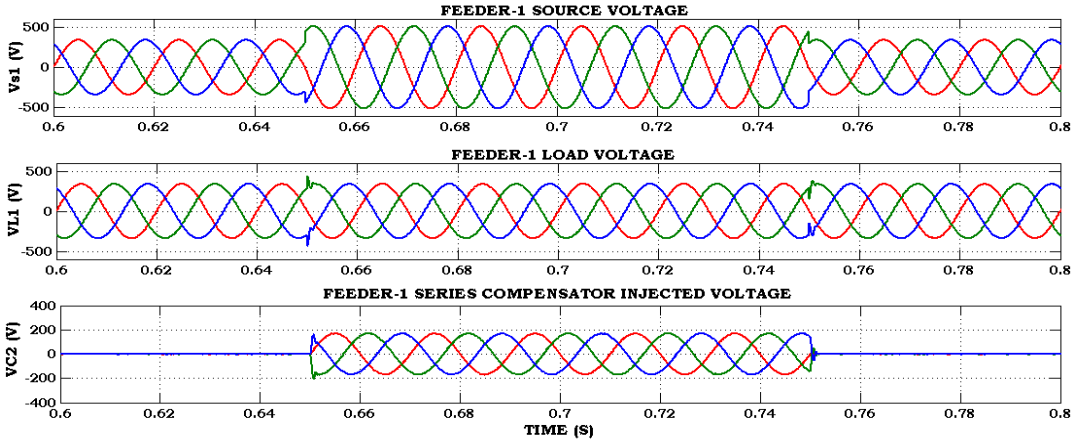

Figure 13. Simulation outcomes of voltage-swell compensation in feeder-1 using FLC-based SRF-controlled VSI-1 of the MT-IUPQC device

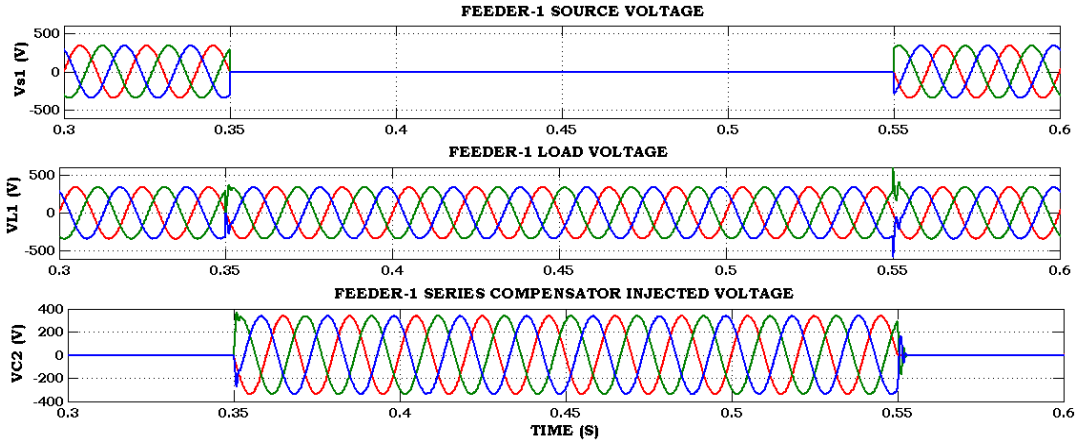

Figure 14. Simulation outcomes of voltage-interruption compensation in feeder-1 using FLC-based SRF-controlled VSI-1 of the MT-IUPQC device

3.2. Compensation of voltage/current concerns in feeder-2 using FLC-based SRF/IRP-controlled MT-IUPQC device

The simulation outcomes of the current compensation in feeder-2 using FLC-based IRP-controlled VSI-4 of the MT-IUPQC device is depicted in Figure 15. In this case, the feeder-2 of the multi-feeder distribution network is energized with a voltage of 415 Vrms, 50 Hz for driving the sensitive non-linear load. This sensitive non-linear load produces the uneven harmonic currents into the PCC of feeder-2. Due to these harmonic distortions, feeder-2 has been damaged, resulting in loss of control in the system. Then the shunt VSI-4 of MT-IUPQC in feeder-2 mitigates the harmonic distortions in source current, which is operated as in-phase opposition compensation principle is shown in Figure 15. Figure 16 shows the current THD spectrum analysis in feeder-2: the THD of non-linear sensitive load current is 30.05% as in Figure 16(a), and the recovered THD of source current is 2.71% as in Figure 16(b), which is well within IEEE-519/2014 norms. The FLC-IRP controller always maintains DC-link voltage as the specified voltage value of 880 V is depicted in Figure 17, and also the source current of feeder-1 is always in-phase with the source voltage, which represents the unity power-factor is shown in Figure 18. The simulation outcomes of voltage compensation in feeder-2 using FLC-based SRF-controlled VSI-3 of the MT-IUPQC device is depicted in Figures 19 and 20. In this case, the feeder-2 of the multi-feeder distribution network is energized with a voltage of 415V rms, 50Hz for driving the sensitive non-linear load. This sensitive non-linear load is affected by several voltage issues. Similarly, the VSI-3 of MT-IUPQC mitigates the voltage sag and voltage swell in feeder-2 are shown in Figures 19 and 20, respectively. The obtained results show that the feeder-2 becomes sinusoidal in nature, linearly, balancing and fundamental factor, and delivers quality power and reliable power to consumer loads.

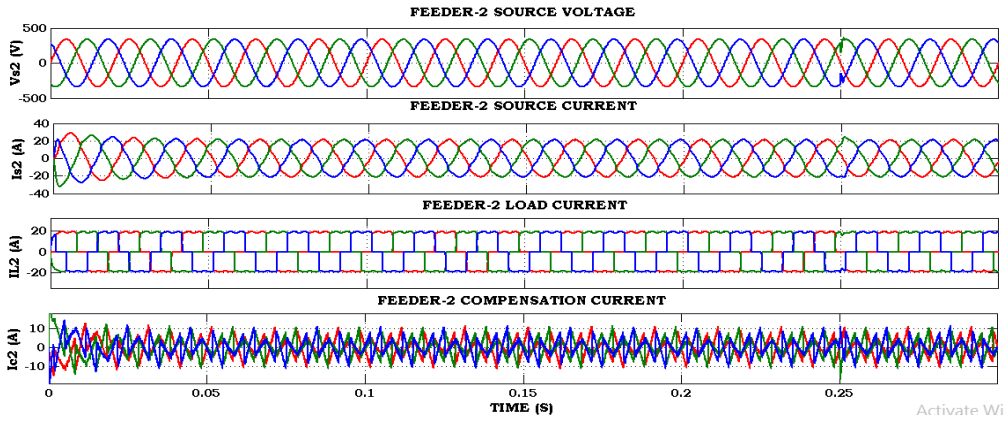

Figure 15. Simulation outcomes of current compensation in feeder-2 using FLC-based IRP-controlled VSI-4 of the MT-IUPQC device

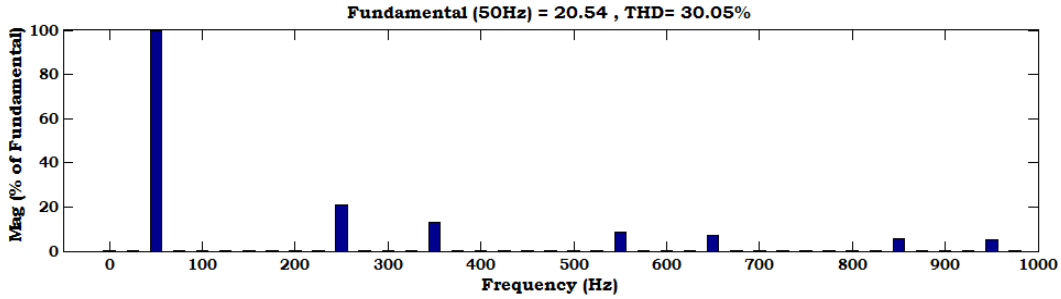

(a)

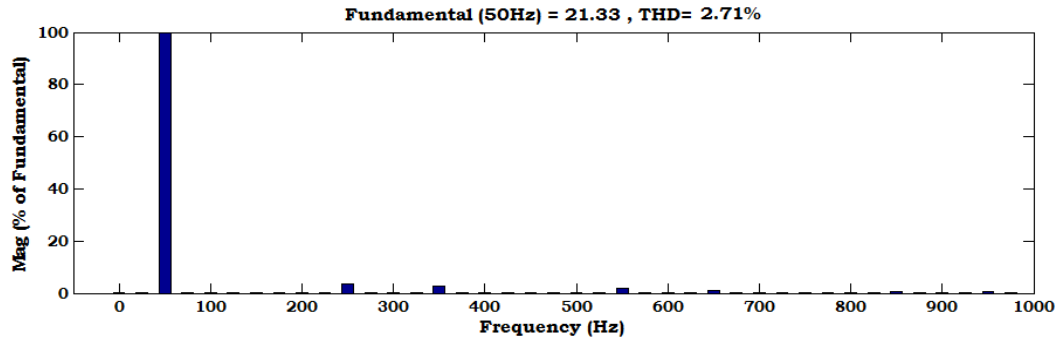

(b)

Figure 16. Current THD spectrum analysis in feeder-2 (a) THD of non-linear sensitive load current and (b) THD of source current

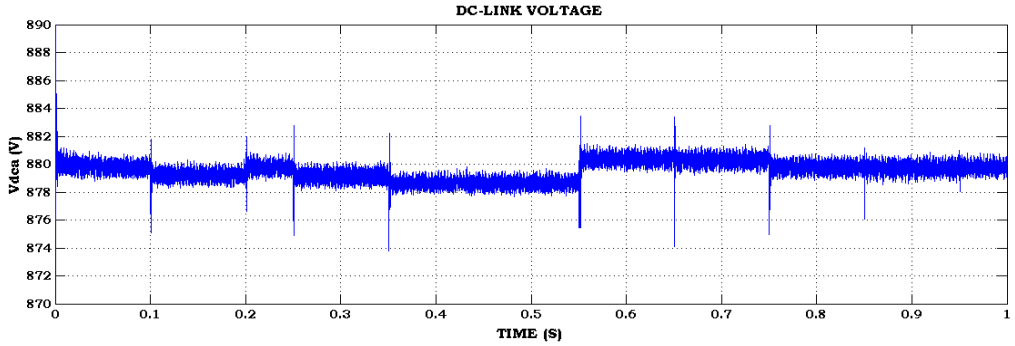

Figure 17. DC-link capacitor voltage

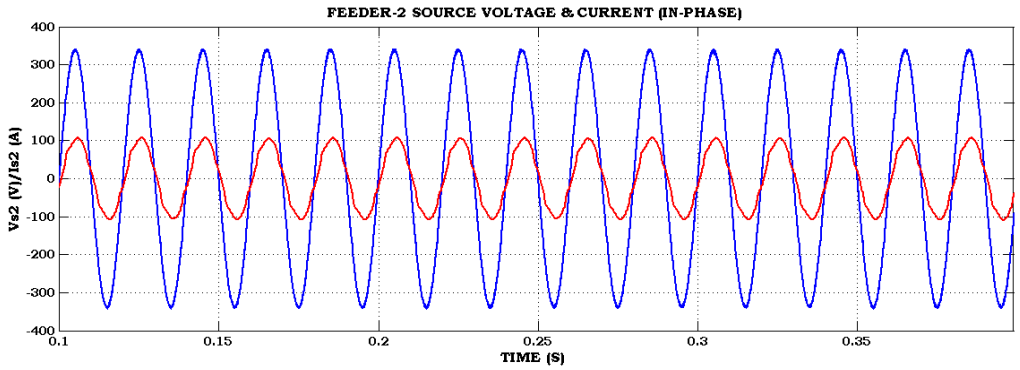

Figure 18. Source voltage and current (in-phase)

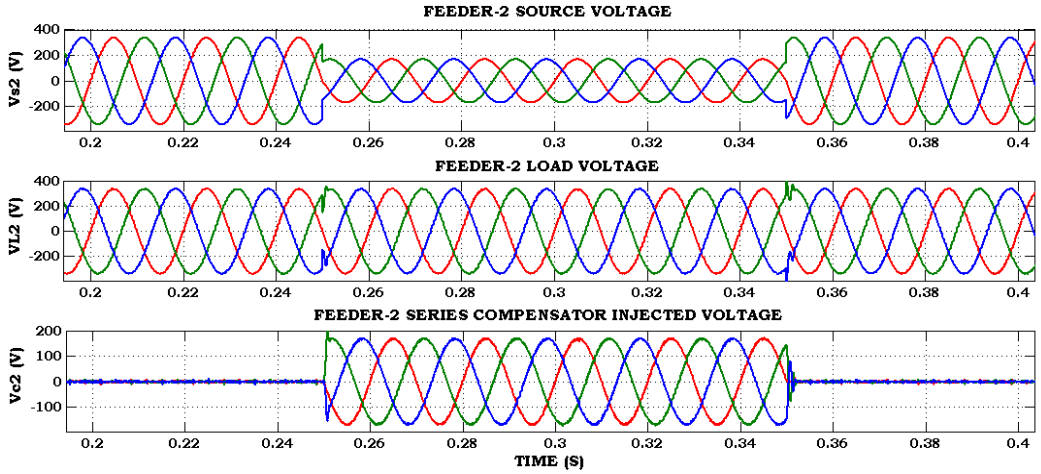

Figure 19. Simulation outcomes of voltage-sag compensation in feeder-2 using FLC-based SRF-controlled VSI-3 of the MT-IUPQC device

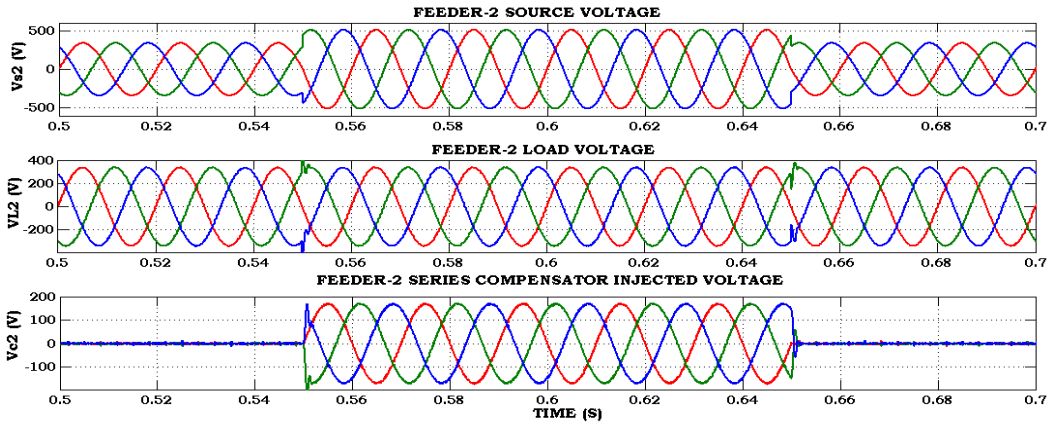

Figure 20. Simulation outcomes of voltage-swell compensation in feeder-2 using FLC-based SRF-controlled VSI-3 of the MT-IUPQC device

The comparisons and bar-graph representation of voltage THD of source voltage, sensitive load-side voltage in a feeder-2 of multi-feeder system is presented in Table 3 and Figure 21. The comparisons and bar-graph representation of non-linear sensitive load current, source/PCC current in feeder-1 and 2 are presented in Tables 4 and 5, Figures 22 and 23, respectively. The illustration of voltage values of source, sensitive load, and VSI-1 and 3 injected voltage in feeder-1 and 2 is presented in Tables 6 and 7.

Table 3. Comparisons of voltage THD of source voltage, sensitive load-side voltage in feeder-2 of multi-feeder system

Method	Source voltage THD (%)	Sensitive load voltage THD (%)
No compensation	20.68	20.68
PI-SRF Fed MT-IUPQC [13]	20.62	0.52
FLC-SRF Fed MT-IUPQC	20.62	0.43

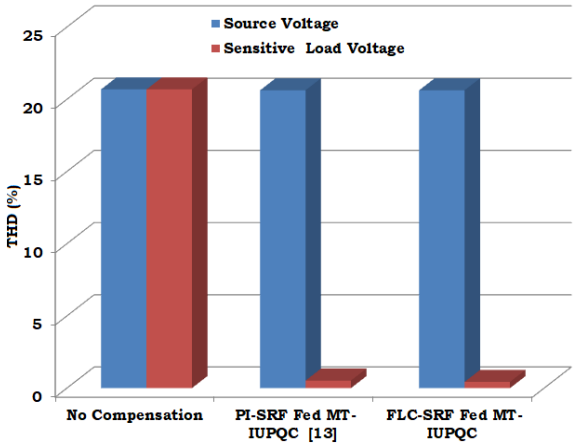

Figure 21. Bar-graph representation of voltage THD comparisons in feeder-2

Table 4. Comparisons of non-linear sensitive load current, source/PCC current in feeder-2 of multi-feeder system

Method	Non-linear sensitive load current THD (%)	Source current THD (%)
No compensation	30.07	30.07
PI-IRP Fed MT-IUPQC [14]	30.05	5.20
FLC-IRP Fed MT-IUPQC	30.05	2.71

Table 5. Comparisons of non-linear sensitive load current, source/PCC current in feeder-1 of multi-feeder system

Method	Non-linear sensitive load current THD (%)	Source current THD (%)
No compensation	30.19	30.19
PI-IRP Fed MT-IUPQC [14]	30.19	5.20
FLC-IRP Fed MT-IUPQC	30.19	2.45

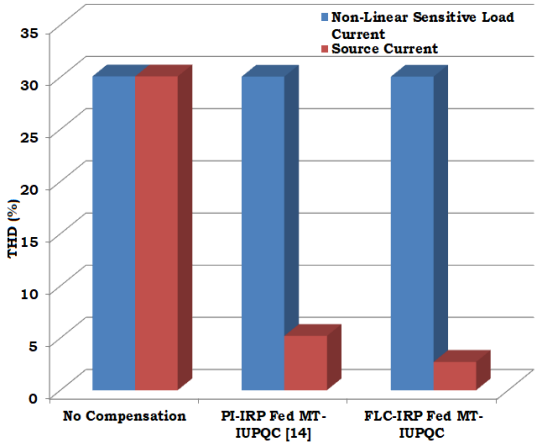

Figure 22. Bar-graph representation of current THD comparisons in feeder-2

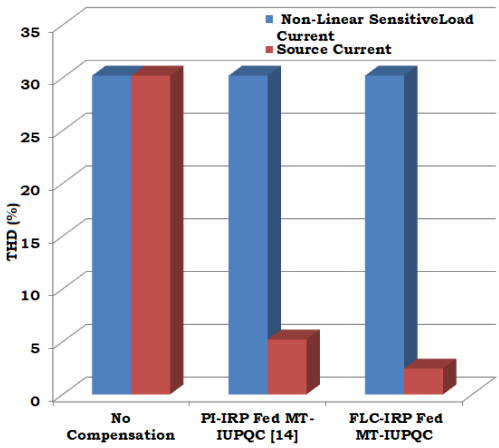

Figure 23. Bar-graph representation of current THD comparisons in feeder-1

Table 6. Voltage values of source, sensitive load, and VSI-1 injected voltage in feeder-1

Operating condition	Source voltage (V)	VSI-1 injected voltage (V)	Non-linear sensitive load voltage (V)
Under normal case (before t-0.1 sec)	340	0	340
Under voltage-sag (0.1 < t <0.2 sec)	170	+170	340
Under voltage-interruptions (0.35 < t <0.55 sec)	0	+340	340
Under voltage-swell (0.65 < t <0.75 sec)	510	-170	340

Table 7. Voltage values of source, sensitive load, and VSI-3 injected voltage in feeder-2

Operating condition	Source voltage (V)	VSI-3 injected voltage (V)	Non-linear sensitive load voltage (V)
Under normal case (before t-0.25 sec)	340	0	340
Under voltage-sag (0.25 < t <0.35 sec)	170	+170	340
Under voltage-swell (0.55 < t <0.65 sec)	510	-170	340

4. CONCLUSION

In this work, the working and performance of the FLC-controlled SRF/IRP-controlled MT-IUPQC device are presented. The FLC-controlled MT-IUPQC works very well for compensation of various current/voltage-driven PQ issues in a multi-feeder network. The proposed FLC exhibits an intelligent, knowledge-driven approach that incorporates FLC membership functions and fuzzy logic rule structure. These components are crucial components of fuzzy controllers; they provide the intelligent knowledge set with subjective assessments for improved mitigation of PQ difficulties. The obtained THD of source current is 2.45%, 2.71%, which is substantially within IEEE-519/2014 limits and much lower than the THD of non-linear sensitive load current is 30.19%, 30.05% in both feeders-1 and 2. Similarly, the THD of non-linear sensitive load voltage is 0.43%, which is considerably within IEEE-519/2014 requirements and significantly lower than the THD of the voltage source, which was measured at 20.62% in feeder 1.

FUNDING INFORMATION

Authors state no funding involved.

AUTHOR CONTRIBUTIONS STATEMENT

This journal uses the Contributor Roles Taxonomy (CRediT) to recognize individual author contributions, reduce authorship disputes, and facilitate collaboration.

Name of Author	C	M	So	Va	Fo	I	R	D	O	E	Vi	Su	P	Fu
Venna Jaya Lakshmi	✓	✓	✓	✓	✓	✓		✓	✓	✓	✓		✓	✓
Katragadda Swarnasri		✓		✓		✓	✓	✓		✓	✓	✓	✓	

C : **C**onceptualization
M : **M**ethodology
So : **So**ftware
Va : **Va**lidation
Fo : **Fo**rmal analysis
I : **I**nvestigation
R : **R**esources
D : **D**ata Curation
O : Writing - **O**riginal Draft
E : Writing - Review & **E**diting
Vi : **Vi**sualization
Su : **Su**pervision
P : **P**roject administration
Fu : **Fu**nding acquisition

CONFLICT OF INTEREST STATEMENT

The author declares that there are no known conflicts of interest associated with this publication. There are no financial or personal relationships that could inappropriately influence or bias the content of this work.

INFORMED CONSENT

Not applicable. This study did not involve human participants, human data, or any personally identifiable information. All data used were either publicly available, fully anonymized, or derived from non-human sources, and therefore no informed consent was required from individuals.

ETHICAL APPROVAL

Not applicable. This research did not involve human subjects, human biological materials, or experimental procedures on animals. The work was conducted solely on computational models, publicly available datasets, or non-sensitive data that did not require intervention with living organisms. Therefore, ethical approval from an institutional review board or animal ethics committee was not necessary for this study.

DATA AVAILABILITY

Data availability is not applicable to this paper as no new data were created or analyzed in this study.

REFERENCES

[1] J. Yaghoobi, A. Abdullah, D. Kumar, F. Zare, and H. Soltani, "Power quality issues of distorted and weak distribution networks in mining industry: a review," *IEEE Access*, vol. 7, pp. 162500–162518, 2019, doi: 10.1109/ACCESS.2019.2950911.

[2] X. P. Zhang and Z. Yan, "Energy quality: a definition," *IEEE Open Access Journal of Power and Energy*, vol. 7, pp. 430–440, 2020, doi: 10.1109/OAJPE.2020.3029767.

[3] T. Tarasiuk *et al.*, "Review of power quality issues in maritime microgrids," *IEEE Access*, vol. 9, pp. 81798–81817, 2021, doi: 10.1109/ACCESS.2021.3086000.

[4] E. Hossain, M. R. Tur, S. Padmanaban, S. Ay, and I. Khan, "Analysis and mitigation of power quality issues in distributed generation systems using custom power devices," *IEEE Access*, vol. 6, pp. 16816–16833, 2018, doi: 10.1109/ACCESS.2018.2814981.

[5] S. Singh and S. S. Letha, "Various custom power devices for power quality improvement: a review," in *2018 International Conference on Power Energy, Environment and Intelligent Control, PEEIC 2018*, 2018, pp. 689–695, doi: 10.1109/PEEIC.2018.8665470.

[6] J. R. -Perez, A. G. -Cerrada, M. O. -Gimenez, and J. L. Z. -Macho, "On the power flow limits and control in series-connected custom power devices," *IEEE Transactions on Power Electronics*, vol. 31, no. 10, pp. 7328–7338, Oct. 2016, doi: 10.1109/TPEL.2015.2509003.

[7] M. Zhang *et al.*, "Multiport current-limiting interline dynamic voltage restorer for power quality enhancement in renewable DC microgrid," *IEEE Journal of Emerging and Selected Topics in Power Electronics*, vol. 14, no. 2, pp. 1710–1723, Apr. 2025, doi: 10.1109/JESTPE.2025.3612918.

[8] L. Gyugyi, "Interline power flow controller (IPFC)," in *Advanced Solutions in Power Systems: HVDC, FACTS, and AI Techniques*, IEEE, 2016, pp. 629–649, doi: 10.1002/9781119175391.ch11.

[9] G. Mythily and S. V. R. L. Kumari, "Power quality improvement by IUPQC," in *Proceedings of the International Conference on Inventive Research in Computing Applications, ICIRCA 2018*, 2018, pp. 1280–1285, doi: 10.1109/ICIRCA.2018.8597191.

[10] A. K. Yadav, P. Tiwari, and R. Maurya, "Power quality conditioning in multifeeder using MC-UPQC," in *2020 International Conference on Electrical and Electronics Engineering (ICE3)*, Gorakhpur, India, pp. 645–649, doi: 10.1109/ICE348803.2020.9122992.

[11] G. Satyanarayana, K. N. V. Prasad, G. R. Kumar, and K. L. Ganesh, "Improvement of power quality by using hybrid fuzzy controlled based IPQC at various load conditions," in *2013 International Conference on Energy Efficient Technologies for Sustainability, ICEETS 2013*, 2013, pp. 1243–1250, doi: 10.1109/ICEETS.2013.6533565.

[12] G. Satyanarayana, K. L. Ganesh, C. N. Kumar, and M. V. Krishna, "A critical evaluation of power quality features using hybrid multi-filter conditioner topology," in *2013 International Conference on Green Computing, Communication and Conservation of Energy, ICGCE 2013*, 2013, pp. 731–736, doi: 10.1109/ICGCE.2013.6823530.

[13] K. B. Rai, N. Kumar, and A. Singh, "PV integrated UPQC for power quality improvement based on MAF-SRF," in *2022 IEEE Silchar Subsection Conference, SILCON 2022*, 2022, pp. 1–7, doi: 10.1109/SILCON55242.2022.10028949.

[14] V. Gundeboina, R. R. Chilipi, and S. Arya, "Power quality enhancement using UPQC-S with multiple adaptive noise cancellation filters," in *2022 IEEE 2nd International Conference on Sustainable Energy and Future Electric Transportation, SeFeT 2022*, 2022, pp. 1–5, doi: 10.1109/SeFeT55524.2022.9909174.

[15] J. V. Lakshmi and L. S. Rao, "Power quality improvement using intelligent fuzzy-VLLMS based shunt active filter," *International Journal of Recent Technology and Engineering*, vol. 8, no. 6, pp. 1004–1012, Mar. 2020, doi: 10.35940/ijrte.f7372.038620.

[16] K. Sarita *et al.*, "Power enhancement with grid stabilization of renewable energy-based generation system using UPQC-FLC-EVA technique," *IEEE Access*, vol. 8, pp. 207443–207464, 2020, doi: 10.1109/ACCESS.2020.3038313.

[17] M. Prasad, Y. K. Nayak, R. R. Shukla, R. Peesapati, and S. Mehera, "Design and analysis of renewable-energy-fed UPQC for power quality improvement," in *Energy Systems in Electrical Engineering*, Singapore: Springer, 2022, pp. 107–124, doi: 10.1007/978-981-19-0979-5_6.

[18] S. S. N. L. Bhavani and L. S. Rao, "Realization of novel multi-feeder UPQC for power quality enhancement using proposed hybrid fuzzy+PI controller," in *2019 Innovations in Power and Advanced Computing Technologies (i-PACT)*, 2019, doi: 10.1109/i-PACT44901.2019.8960156.

[19] R. K. Israni, R. Yadav, R. Singh, and B. R. Reddy, "Power quality enhancement in wind-hydro based hybrid renewable energy system by interlocking of UPQC," in *2023 3rd International Conference on Energy, Power and Electrical Engineering (EPEE)*, Sep. 2023, pp. 112–123, doi: 10.1109/EPEE59859.2023.10352036.

[20] A. Heenkenda, A. Elsanabary, M. Seyedmahmoudian, S. Mekhilef, A. Stojcevski, and N. F. A. Aziz, "Unified power quality conditioners based different structural arrangements: a comprehensive review," *IEEE Access*, vol. 11, pp. 43435–43457, 2023, doi: 10.1109/ACCESS.2023.3269855.

[21] K. Saleh and N. Hantouli, "A photovoltaic integrated unified power quality conditioner with a 27-level inverter," *TELKOMNIKA (Telecommunication Computing Electronics and Control)*, vol. 17, no. 6, pp. 3232–3248, 2019, doi: 10.12928/TELKOMNIKA.v17i6.13224.

[22] K. L. Ganesh, N. S. Naik, K. Narendra, and G. S. Narayana, "A newly designed asymmetrical multi-cell cascaded multilevel inverter for distributed renewable energy resources," *International Journal of Recent Technology and Engineering*, vol. 7, pp. 248–255, 2019.
[23] J. R. G. -Martínez, E. E. C. -Miguel, R. V. C. -Serrano, F. M. -Mondragón, M. T. -Ayala, and J. R. -Reséndiz, "A PID-type fuzzy logic controller-based approach for motion control applications," *Sensors*, vol. 20, no. 18, pp. 1–19, 2020, doi: 10.3390/s20185323.
[24] G. Satyanarayana and K. L. Ganesh, "Tuning a robust performance of adaptive fuzzy-PI driven DSTATCOM for non-linear process applications," in *Swarm, Evolutionary, and Memetic Computing*, Cham, Switzerland: Springer, 2015, pp. 523–533, doi: 10.1007/978-3-319-20294-5_46.
[25] A. Sakalli, T. Kumbasar, and J. M. Mendel, "Towards systematic design of general type-2 fuzzy logic controllers: analysis, interpretation, and tuning," *IEEE Transactions on Fuzzy Systems*, vol. 29, no. 2, pp. 226–239, Feb. 2021, doi: 10.1109/TFUZZ.2020.3016034.
[26] A. N. K. Nasir, M. A. Ahmad, and M. O. Tokhi, "Hybrid spiral-bacterial foraging algorithm for a fuzzy control design of a flexible manipulator," *Journal of Low Frequency Noise Vibration and Active Control*, vol. 41, no. 1, pp. 340–358, 2022, doi: 10.1177/14613484211035646.
[27] R. Luca, M. Whiteley, T. Neville, P. R. Shearing, and D. J. L. Brett, "Comparative study of energy management systems for a hybrid fuel cell electric vehicle - a novel mutative fuzzy logic controller to prolong fuel cell lifetime," *International Journal of Hydrogen Energy*, vol. 47, no. 57, pp. 24042–24058, 2022, doi: 10.1016/j.ijhydene.2022.05.192.

BIOGRAPHIES OF AUTHORS

Venna Jaya Lakshmi completed her B.Tech. from Potti Sri Ramulu Engineering College, Vijayawada, in 2013 and M.Tech. from PVP Siddhartha Institute of Technology in 2015. Currently pursuing a Ph.D. as a research scholar in the Department of Electrical Engineering, Acharya Nagarjuna University, Andhra Pradesh, India. She has authored or coauthored more than 10 publications, including international conferences and journals, with good citations. His research interests include power systems, power-quality improvement, FACTS, electric vehicles, CPC techniques, power electronics, distributed generation, renewable energy sources, and control systems. She can be contacted at email: vennajayalakshmi.eee@gmail.com.

Dr. Katragadda Swarnasri is presently working as a professor in the Department of Electrical and Electronics Engineering at R.V.R & J.C. College of Engineering, Guntur. She completed her B.Tech. (Electrical and Electronics Engineering) in 1999 from R.V.R & J.C. College of Engineering and M.Tech. (Power Systems Engineering) in 2001 from REC, Warangal. She obtained her Ph.D. degree from Jawaharlal Nehru Technological University, Hyderabad, in 2015. She published more than 35 journals and conference papers in her research areas of electrical power systems, power quality, energy audit and conservation, renewable energy, smart grids, and AI techniques. She is a member of IEEE and is involved with IEEE activities as a volunteer under IEEE Guntur subsection. She can be contacted at email: swarnasrik@rvrjc.ac.in.